Research article

Contrasting microscopic interactions determine the properties of water/methanol solutions

Carmelo Corsaro[1,2,†], **Francesco Mallamace**[1,2,3,4], **Sebastiano Vasi**[2],
Sow-Hsin Chen[3], **H. Eugene Stanley**[4], **Domenico Mallamace**[5]

[1] *CNR-IPCF Messina, Istituto per i Processi Chimico-Fisici, Viale F. Stagno D'Alcontres 37, 98158 Messina, Italy*
[2] *Dipartimento MIFT, Sezione di Fisica, Università di Messina, Viale F. Stagno D'Alcontres 31, 98166 Messina, Italy*
[3] *Department of Nuclear Science and Engineering, Massachusetts Institute of Technology, Cambridge, MA 02139, USA*
[4] *Center for Polymer Studies and Department of Physics, Boston University, Boston, MA 02215, USA*
[5] *Consorzio interuniversitario per lo sviluppo dei Sistemi a Grande Interfase - CSGI,*
Via della Lastruccia 3, 50019 Sesto Fiorentino, Firenze, Italy
Corresponding author. E-mail: [†] *ccorsaro@unime.it*
Received February 24, 2017; accepted April 14, 2017

Herein we study the different microscopic interactions occurring in water/methanol solutions at different methanol molar fractions, using NMR spctroscopy. Temperature was found to determine which interaction dominates. It was found that the mixing between water and methanol is non-ideal because of the presence of interactions like hydrophobicity and hydrophilicity. These results indicate that the competition between hydrophilic and hydrophobic interactions is different in different thermal regions, and that the physical properties of the solution are determined by the character of the solution itself, which in turn depends on the mole fraction of methanol and on the temperature.

1 Introduction

A binary mixture of two components is ideal when its physical properties change linearly with changing molar concentration. Although this holds for solutions of simple liquids, a mixture of water and methanol is non-ideal, and the degree of its non-ideality is determined by thermodynamical variables like temperature and pressure. Liquid methanol is arranged in one- and two-dimensional hydrogen bond (HB) networks [1, 2], but liquid water forms three-dimensional HB networks [3]. This non-ideal mixing occurs because of strong interactions between the molecules of the two liquids. Methanol is the smallest amphiphilic molecule, consisting of a single hydrophilic (OH) and a single hydrophobic (CH_3) group. When methanol is added to water, both hydrogen bonding and non-polar interactions are observed [4–7].

The competition between these two interactions depends on the temperature and the composition of the mixture. Understanding the behavior of water molecules interacting with amphiphilic molecules, and of the corresponding thermal regimes, is essential for understanding the complex biological processes involving water [8, 9].

Water/methanol mixtures have been extensively studied. In 1935, Gibson found that the compressibility minimum is a function of the concentration of methanol in water and hypothesized that the presence of methanol, unlike other types of solutes, favored the increased association of water molecules [10]. In 1943, Frank and Evans hypothesized that normal water structure is significantly enhanced by hydrophobicity, producing a more ordered "iceberg-like" structure near the methyl headgroup [11]. This hypothesis of hydrophobic enhancement of water structuring has been extensively debated since [7, 11–13] and has been linked to the corresponding increase in enthalpy during hydrogen-bond formation [6, 11] and entropy loss — as in protein folding [14].

In these mixtures, structural inhomogeneities were observed on a microscopic length scale, which have thermodynamic and dynamic effects. Particularly, changing the temperature generates different kinds of clusters [15], and the conditions for micro-segregation have been deter-

---

*Special Topic: Water and Water Systems (Eds. F. Mallamace, R. Car, and Limei Xu).

mined for water/methanol mixtures [4, 16–18]. Neutron scattering and X-ray absorption spectroscopy analyses have revealed different local water structures around the methyl group of methanol for different mixture compositions [19, 20]. In particular, at a high methanol mole fraction ($X_M \geq 0.7$), few water molecules can form HBs with methanol hydroxyl groups or stabilize the mixture by pushing the methyl groups toward each other. At an intermediate methanol mole fraction ($0.7 > X_M > 0.3$), mixed three-dimensional HB clusters form and lead to the well-known extreme values of thermodynamic parameters [6, 12, 13, 15, 21–23]. In contrast, at a high water mole fraction ($X_M \leq 0.3$), methanol molecules are individually embedded in the water HB network and produce a slight compressive effect [19, 20].

A recent study of the relaxation times of water/ methanol mixtures revealed opposing behaviors in two thermal regimes [6]. In the low-T regime below the so-called fragile-to-strong crossover in water, the dynamics of the solution is dominated by the presence of low-density-liquid (LDL) structures, indicating the occurrence of a liquid-liquid phase transition in water [24–26]. This corresponds to an onset of dynamical heterogeneities and a decoupling in transport properties, which has a more general, universal importance [27, 28]. In contrast, in the high-T regime, the thermal energy lowers the stability of hydrogen bonding, and the hydrophobicity control of the methanol in the solution increases [6]. The border temperature of this effect is ≈ 320 K, corresponding to the temperature above which water behaves as a simple liquid [29–31]. In contrast, the onset temperature of complete LDL dominance is the same as the temperature of the so-called Widom line for water [24, 32] and depends on the concentration of the solution [6].

The competition between these two different kinds of interactions (during which, pathways within the corresponding energy landscape are selected) governs most biological processes, such as protein folding/unfolding [33].

Herein we use nuclear magnetic resonance (NMR) spectroscopy to separately probe the dynamics of hydroxyl and methyl groups because the spectrum of corresponding resonance frequencies is well-resolved. We report the NMR spectroscopy results for water/methanol mixtures to distinguish between the hydrophilic and hydrophobic contributions and to determine their different abilities to control the solution properties.

2   Materials and methods

Using a Bruker Avance spectrometer operating at 700-MHz ^{1}H resonance Frequency, we performed NMR experiments under 1 atm pressure. We use ultra- gradient pure water and super-purity methanol, both supplied by Romil pure chemistry [15]. Experiments were performed at temperatures up to 310 K and down to the occurrence of mixture solidification. The temperature was calibrated by means of the standard reference with an accuracy of 0.2 K [15].

The proton chemical shifts and the relaxation times for the mixtures were obtained for methanol mole fractions X_M of 0.1, 0.24, 0.5, and 0.7. In particular, we examined the dynamical and structural data obtained from an analysis of the longitudinal component, i.e., the spin-lattice (T_1), the transverse component, i.e., the spin–spin (T_2) of proton magnetization, and the proton chemical shift δ.

Using NMR spectroscopy, we separately followed the signals of the three functional groups in solution: hydroxyls from water (OH_W) and methanol (OH_M) and methyl from methanol (CH_3). The details of the pulse sequences and the corresponding parameters used to obtain the proton NMR spectra and to measure the relaxation times are described in Refs. [13, 15]. We have extended our previous experiments and interpreted the results obtained in the framework of microscopic interactions described by a single correlation time τ_c. Dipolar relaxation is the most important relaxation mechanism between protons in liquids and it can be expressed in terms of a rotational motion characterized by a specific correlation time τ_c [34]. When the fractions of dipolar contribution to the spin-lattice and spin–spin relaxation mechanisms are the same, both corresponding equations depend on the same rotational correlation time τ_c [35–37]. The details for the spin-lattice relaxation time are

$$R_1 = \frac{1}{T_1} = \frac{A}{r^6}\left(\frac{\tau_c}{1+\omega_0^2\tau_c^2} + \frac{4\tau_c}{1+4\omega_0^2\tau_c^2}\right), \quad (1)$$

and for the spin–spin relaxation time they are

$$R_2 = \frac{1}{T_2} = \frac{A}{2r^6}\left(3\tau_c + \frac{5\tau_c}{1+\omega_0^2\tau_c^2} + \frac{2\tau_c}{1+4\omega_0^2\tau_c^2}\right), \quad (2)$$

where A is a constant equal to $3\gamma^4\hbar^2/10$ (γ is the proton gyromagnetic ratio and $\hbar$ the Plank constant divided by 2π), r is the interproton distance, and ω_0 the proton Larmor frequency. Dividing Eq. (1) by Eq. (2) gives an equation for the determination of τ_c,

$$12B\left(\omega_0\tau_c\right)^4 + (37B-8)\left(\omega_0\tau_c\right)^2 + 10B - 5 = 0, \quad (3)$$

where B is $T_2/(2T_1)$. Thus we calculate τ_c by measuring both T_1 and T_2, which helps us better understand the dynamics of the molecule. By following the relaxations of the three functional groups separately, we better understand both the hydrophilic and hydrophobic correlations. Furthermore, the trend of the chemical shift provides insight into the properties of the local structures forming within the solutions.

3 Results and discussion

Figure 1 shows the proton NMR spectra of water/methanol solutions with $X_M = 0.5$ at different temperatures (205 K $< T <$ 310 K). The spectra show three signals that change differently with temperature. Lowering the temperature shifts the methyl signal toward the high-field region, while lowering the temperature shifts both hydroxyl signals toward the low-field region. In other words, the hydroxyl groups are more structured at low temperatures and the methyl groups are more structured at high temperatures.

The changes in the difference between the chemical shifts of the OH_W and CH_3 groups occur because of variations in the water HB network and hydrogen bond strength. At low temperatures, this difference in chemical shift has a linear dependence on the methanol mole fraction. At high temperatures, the structurally induced hydrophobic effect causes a rounding off at a methanol mole fraction of ≈ 0.1 [13]. On the other hand, the difference between the chemical shifts of the OH_M and OH_W groups $\delta(OH_M - OH_W)$ is apparently temperature-independent but is not. In fact, a careful analysis reveals measurable differences on the order of hundredths of ppm, indicating an interesting temperature-dependent trend.

Figure 2 shows a three-dimensional plot of the thermal behavior of the relative proton chemical shifts between the hydroxyl groups in the mixture, $\delta(OH_M - OH_W)$, at different methanol mole fractions. The maximum values for the relative chemical shift at each methanol mole fraction (solid red line) indicates that there is a temperature at which the hydroxyl peaks are most separated on the spectra. Furthermore, this temperature assumes a max-
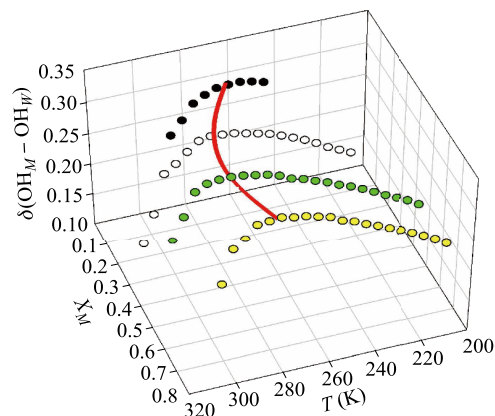
Fig. 2 Trend of the proton relative chemical shift between hydroxyl groups within the mixture. There is a temperature of maximum distance between hydroxyl peaks that depends on the mixture composition showing a maximum at $X_M \simeq 0.45$.

imum value at a mixture composition of $X_M \simeq 0.45$. This confirms that at this intermediate composition, the mixture is a bi-percolating one that indicates maximum immiscibility.

Figure 2 shows that when $\delta(OH_M - OH_W)$ is zero, i.e., when the two peaks coalesce at $T > 300$ K for $X_M = 0.1$ (black circles), the two hydroxyl groups have the same chemical environment and undergo rapid chemical exchange — the larger the distance between their peaks, the larger is the probability that they are poorly correlated or randomly mixed.

The behavior of $\delta(OH_M - OH_W)$ as a function of temperature is similar at all methanol mole fractions, i.e., the temperature is the strongest control parameter for water/methanol solutions within the studied concentration range. The different maximum temperatures for different methanol mole fractions suggests that the longest distance between the OH_M and OH_W groups at different temperatures is weakly dependent on concentration. Above this maximum temperature, the hydrophobic effect of the methyl groups and the disordering action due to the high temperature reduce the average distances between the hydroxyl groups. At lower temperatures, the hydrophilic effect becomes increasingly strong, and the hydrogen bonds become stronger and more stable.

Figure 1 shows different signal widths related to the spin–spin relaxation time, confirming the fact that the exchange of hydroxyls is rapid only at high temperatures. As stated above, calculating τ_c from T_1 and T_2 using Eq. (3) gives new insights into the dynamics of single molecules in terms of their different molecular groups.

Figure 3 shows the thermal behavior of τ_c for the hydroxyl groups of water and methanol when $X_M = 0.5$. It confirms that the two hydroxyl groups are strongly
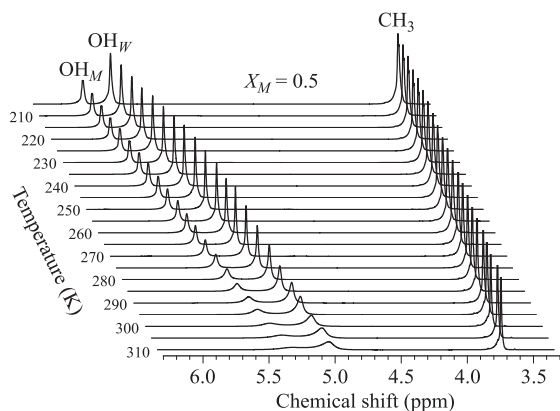

Fig. 1 The proton NMR spectra of water/methanol solutions at different temperature for $X_M = 0.5$. The three peaks are labeled with the molecular group originating the corresponding signal.
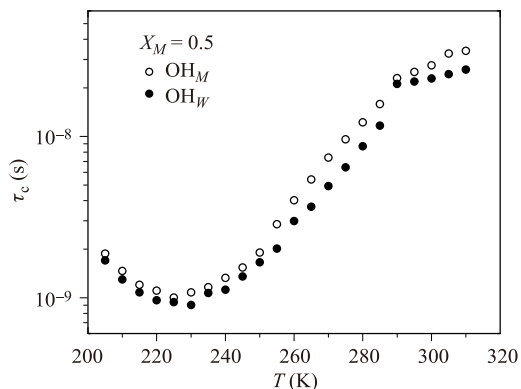
Carmelo Corsaro, et al., Front. Phys. 13(1), 138201 (2018)

Frontiers of Physics

138201-3

Fig. 3 The rotational correlation time τ_c as a function of the temperature for hydroxyl groups of water and methanol at the equimolar composition ($X_M = 0.5$).

correlated and show the same τ_c versus temperature behavior. This correlation time shows a clear minimum at $\approx$ 225 K and a sharp change at $\approx$ 290 K. The temperature of 225 K is also the Widom line temperature for water, at which the correlations between water molecules are maximum, the hydrogen bond network is complete [24, 32], and the correlation is fastest. The temperature of 290 K for the water/methanol solution with $X_M = 0.5$ is close to the corresponding temperature for the maximum distance between hydroxyls. This relatively high temperature falls within the region of stability for both water and methanol and is the temperature at which hydrophilicity no longer dominates hydrophobicity. The onset of hydrophobicity occurs slightly below this temperature. Figure 4 shows the thermal behavior of τ_c for the methyl groups of methanol at the equimolar composition $X_M = 0.5$. The τ_c value of the methyl groups reaches a maximum at $\approx$ 265 K and marks the onset
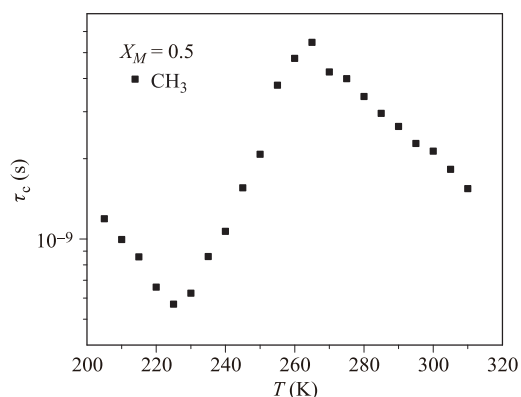

Fig. 4 The rotational correlation time τ_c as a function of the temperature for methyl groups of methanol at the equimolar composition ($X_M = 0.5$).

of the hydrophobic interaction. It reaches its minimum value at $\approx$ 225 K, corresponding to the local correlation maximum for water molecules.

We show the data for $X_M = 0.5$ because this interesting concentration corresponds to an equimolar contribution from the two species in which clustering is apparent [15]. We have performed a more complete and exhaustive study of the NMR correlation time in water/methanol solutions that will be published elsewhere [38]. In particular we have examined the effect of increasing temperature in water and water-based systems, and used the framework of the Bloembergen–Purcell–Pound theory to quantify the thermal behavior of τ_c at different mixture compositions and different dynamical regimes by analyzing the behavior of the proton relaxation times as a function of τ_c [34, 38].

4   Conclusion

In this study, we have used NMR spectroscopy to examine how the structure and dynamics of water/methanol solutions are influenced by hydrophilic and hydrophobic microscopic interactions. The hydrophilic interaction is stronger at low temperatures and the hydrophobic interaction is stronger at high temperatures. We have also examined the dependence on the methanol mole fraction that determines the ratio between hydrophobic and hydrophilic moieties in the mixture. We report in detail the relative value of the chemical shift corresponding to hydroxyl groups as a function of temperature at four different methanol mole fractions, $X_M = 0.1$, 0.24, 0.5, and 0.7. A temperature was recorded, at which the distance between the chemical shift of the two hydroxyl peaks maximizes. This temperature depends on the mixture composition and shows a maximum at $X_M \simeq 0.45$. This confirms the presence of immiscibility at the intermediate mixture compositions.

We have also reported the rotational correlation time values (τ_c) obtained by measuring the longitudinal (T_1) and transverse (T_2) relaxation times in an equimolar mixture for both the hydroxyl and methyl groups. This enables us to estimate the different correlation times corresponding to the two interactions. We find that τ_c for hydroxyl groups at $X_M = 0.5$ shows a clear minimum at $\approx$ 225 K and a sharp change at $\approx$ 290 K. The methyl groups has a maximum correlation time at $\approx$ 265 K and a minimum at $\approx$ 225 K. The temperature of 225 K corresponds to the maximum in the local correlation for water molecules, supporting the existence of the Widom line and the liquid-liquid phase transition in water [39]. The high-temperature interval (265 K $< T <$ 290 K) marks the onset and progressive dominance of the hydrophobic effect, as observed in water confined within hydrophobic

nanotubes [40].

The mole fraction values constituting the border between the different structural and dynamical regimes, which are characterized by the competition between the hydrophilic and hydrophobic interactions, depend on the temperature. Our study confirms that low temperatures favor the formation of three-dimensional HB clusters that are characteristic of water local structures, and that high temperatures favor the formation of one- and two-dimensional local structures that are characteristic of liquid methanol.

References

1. J. H. Guo, Y. Luo, A. Augustsson, S. Kashtanov, J. E. Rubensson, D. K. Shuh, H. Ågren, and J. Nordgren, Molecular structure of alcohol–water mixtures, *Phys. Rev. Lett.* 91(15), 157401 (2003)

2. T. Yamaguchi, K. Hidaka, and A. K. Soper, The structure of liquid methanol revisited: A neutron diffraction experiment at $-80°C$ and $+25°C$, *Mol. Phys.* 96(8), 1159 (1999)

3. R. Ludwig, Water: From clusters to the bulk, *Angew. Chem. Int. Ed.* 40(10), 1808 (2001)

4. A. K. Soper, L. Dougan, J. Crain, and J. L. Finney, Excess entropy in alcohol–water solutions: A simple clustering explanation, *J. Phys. Chem. B* 110(8), 3472 (2006)

5. Y. Zhong, G. L. Warren, and S. Patel, Thermodynamic and structural properties of methanol–water solutions using non-additive interaction models, *J. Comput. Chem.* 29(7), 1142 (2008)

6. F. Mallamace, C. Corsaro, D. Mallamace, C. Vasi, S. Vasi, and H. E. Stanley, Dynamical properties of water-methanol solutions, *J. Chem. Phys.* 144(6), 064506 (2016)

7. R. K. Lam, J. W. Smith, and R. J. Saykally, Communication: Hydrogen bonding interactions in water–alcohol mixtures from X-ray absorption spectroscopy, *J. Chem. Phys.* 144(19), 191103 (2016)

8. F. Mallamace, P. Baglioni, C. Corsaro, S. H. Chen, D. Mallamace, C. Vasi, and H. E. Stanley, The influence of water on protein properties, *J. Chem. Phys.* 141(16), 165104 (2014)

9. F. Mallamace, C. Corsaro, D. Mallamace, S. Vasi, C. Vasi, H. E. Stanley, and S. H. Chen, Some thermodynamical aspects of protein hydration water, *J. Chem. Phys.* 142(21), 215103 (2015)

10. R. E. Gibson, The compressions and specific volumes of aqueous solutions of resorcinol and methanol at 25° and the behavior of water in these solutions, *J. Am. Chem. Soc.* 57(9), 1551 (1935)

11. H. S. Frank and M. W. Evans, Free Volume and Entropy in Condensed Systems III. Entropy in binary liquid mixtures; Partial molal entropy in dilute solutions; Structure and thermodynamics in aqueous electrolytes, *J. Chem. Phys.* 13(11), 507 (1945)

12. Y. Koga, K. Nishikawa, and P. Westh, "Icebergs" or no "icebergs" in aqueous alcohols?: Composition-dependent mixing schemes, *J. Phys. Chem. A* 108(17), 3873 (2004)

13. C. Corsaro, R. Maisano, D. Mallamace, and G. Dugo, ^{1}H NMR study of water/methanol solutions as a function of temperature and concentration, *Physica A* 392(4), 596 (2013)

14. W. Kauzmann, Some factors in the interpretation of protein denaturation, *Adv. Protein Chem.* 14, 1 (1959)

15. C. Corsaro, J. Spooren, C. Branca, N. Leone, M. Broccio, C. Kim, S. H. Chen, H. E. Stanley, and F. Mallamace, Clustering dynamics in water/methanol mixtures: A nuclear magnetic resonance study at 205 K $< T <$ 295 K, *J. Phys. Chem. B* 112(34), 10449 (2008)

16. S. Dixit, J. Crain, W. C. K. Poon, J. L. Finney, and A. K. Soper, Molecular segregation observed in a concentrated alcohol water solution, *Nature* 416(6883), 829 (2002)

17. L. Dougan, R. Hargreaves, S. P. Bates, J. L. Finney, V. Réat, A. K. Soper, and J. Crain, Segregation in aqueous methanol enhanced by cooling and compression, *J. Chem. Phys.* 122(17), 174514 (2005)

18. M. Požar, A. Kerasidou, B. Lovrinčević, L. Zoranić, M. Mijaković, T. Primorac, F. Sokolić, V. Teboul, and A. Perera, The microscopic structure of cold aqueous methanol mixtures, *J. Chem. Phys.* 145(14), 144502 (2016)

19. L. Dougan, S. P. Bates, R. Hargreaves, J. P. Fox, J. Crain, J. L. Finney, V. Reat, and A. K. Soper, Methanol-water solutions: A bi-percolating liquid mixture, *J. Chem. Phys.* 121(13), 6456 (2004)

20. M. Nagasaka, K. Mochizuki, V. Leloup, and N. Kosugi, Local structures of methanol-water binary solutions studied by soft X-ray absorption spectroscopy, *J. Phys. Chem. B* 118(16), 4388 (2014)

21. H. Schott, Hydration of primary alcohols, *J. Chem. Eng. Data* 14(2), 237 (1969)

22. Z. J. Derlacki, A. J. Easteal, A. V. J. Edge, L. A. Woolf, and Z. J. Roksandic, Diffusion coefficients of methanol and water and the mutual diffusion coefficient in methanol–water solutions at 278 and 298 K, *J. Phys. Chem.* 89(24), 5318 (1985)

Frontiers of Physics

Carmelo Corsaro, et al., Front. Phys. 13(1), 138201 (2018)

138201-5

Frontiers of Physics

23. S. Z. Mikhail and W. R. Kimel, Densities and viscosities of methanol–water mixtures, *J. Chem. Eng. Data* 6(4), 533 (1961)

24. F. Mallamace, C. Corsaro, D. Mallamace, S. Vasi, C. Vasi, and H. E. Stanley, Thermodynamic properties of bulk and confined water, *J. Chem. Phys.* 141, 18C504 (2014)

25. R. S. Singh, J. W. Biddle, P. G. Debenedetti, and M. A. Anisimov, Two-state thermodynamics and the possibility of a liquid–liquid phase transition in supercooled TIP4P/2005 water, *J. Chem. Phys.* 144(14), 144504 (2016)

26. Y. Ni and J. L. Skinner, Evidence for a liquid–liquid critical point in supercooled water within the E3B3 model and a possible interpretation of the kink in the homogeneous nucleation line, *J. Chem. Phys.* 144(21), 214501 (2016)

27. F. Mallamace, C. Branca, C. Corsaro, N. Leone, J. Spooren, S. H. Chen, and H. E. Stanley, Transport properties of glass-forming liquids suggest that dynamic crossover temperature is as important as the glass transition temperature, *Proc. Natl. Acad. Sci. USA* 107(52), 22457 (2010)

28. F. Mallamace, C. Corsaro, H. E. Stanley, D. Mallamace, and S. H. Chen, The dynamical crossover in attractive colloidal systems, *J. Chem. Phys.* 139(21), 214502 (2013)

29. F. Mallamace, C. Corsaro, and H. E. Stanley, A singular thermodynamically consistent temperature at the origin of the anomalous behavior of liquid water, *Sci. Rep.* 2, 993 (2012)

30. P. Gallo, K. Amann-Winkel, C. A. Angell, M. A. Anisimov, F. Caupin, C. Chakravarty, E. Lascaris, T. Loerting, A. Z. Panagiotopoulos, J. Russo, J. A. Sellberg, H. E. Stanley, H. Tanaka, C. Vega, L. Xu, and L. G. M. Pettersson, Water: A tale of two liquids, *Chem. Rev.* 116(13), 7463 (2016)

31. F. Mallamace, C. Corsaro, D. Mallamace, C. Vasi, and H. E. Stanley, The thermodynamical response functions and the origin of the anomalous behavior of liquid water, *Faraday Discuss.* 167, 95 (2013)

32. L. Xu, P. Kumar, S. V. Buldyrev, S. H. Chen, P. H. Poole, F. Sciortino, and H. E. Stanley, Relation between the Widom line and the dynamic crossover in systems with a liquid–liquid phase transition, *Proc. Natl. Acad. Sci. USA* 102(46), 16558 (2005)

33. F. Mallamace, C. Corsaro, D. Mallamace, S. Vasi, C. Vasi, P. Baglioni, S. V. Buldyrev, S. H. Chen, and H. E. Stanley, Energy landscape in protein folding and unfolding, *Proc. Natl. Acad. Sci. USA* 113(12), 3159 (2016)

34. N. Bloembergen, E. M. Purcell, and R. V. Pound, Relaxation effects in nuclear magnetic resonance absorption, *Phys. Rev.* 73(7), 679 (1948)

35. W. R. Carper, Direct determination of quadrupolar and dipolar NMR correlation times from spin-lattice and spin–spin relaxation rates, *Concepts in Magnetic Resonance Part A* 11(1), 51 (1999)

36. A. Yılmaz, M. Z. Köylü, and H. Budak, Estimation of τ value in proton NMR relaxation times of dibenzo diaza 18-crown–6 ether derivative in solution, *Chem. Phys. Lett.* 427(4–6), 346 (2006)

37. F. Mallamace, C. Corsaro, D. Mallamace, S. Vasi, and H. E. Stanley, NMR spectroscopy study of local correlations in water, *J. Chem. Phys.* 145(21), 214503 (2016)

38. F. Mallamace, C. Corsaro, D. Mallamace, S. Vasi, S.-H. Chen, and H. E. Stanley (submitted)

39. S. Cerveny, F. Mallamace, J. Swenson, M. Vogel, and L. Xu, Confined water as model of supercooled water, *Chem. Rev.* 116(13), 7608 (2016)

40. H. J. Wang, X. K. Xi, A. Kleinhammes, and Y. Wu, Temperature-induced hydrophobic-hydrophilic transition observed by water adsorption, *Science* 322(5898), 80 (2008)

138201-6

Carmelo Corsaro, et al., Front. Phys. 13(1), 138201 (2018)